Article type : Research Article

On the formation of magmatic sulfide systems in the lower crust by long-lived mass transfer through the lithosphere: Insights from the Valmaggia pipe, Ivrea Verbano Zone, Italy

Marek Locmelis[1*], Marilena Moroni[2], Steven W. Denyszyn[3], Laura E. Webb[4], Marco L. Fiorentini[3], Gianluca Sessa[2], Stefano Caruso[3], Ryan Mathur[5], Bolorchimeg Nanzad[1]

[1]Department of Geosciences and Geological and Petroleum Engineering, Missouri University of Science & Technology, Rolla, Missouri, USA.

[2]Dipartimento di Scienze della Terra, Università degli Studi di Milano, Italy

[3]School of Earth Sciences, University of Western Australia, 35 Stirling Highway, Perth, WA 6009, Australia

[4]Department of Geology, University of Vermont, Burlington, Vermont, USA

[5]Juniata College, 1700 Moore St, Huntingdon, Pennsylvania 16652, USA

*corresponding author: Marek Locmelis (locmelism@mst.edu; phone: +1-573-341-4759)

Running head: Sulfide mineralization in the lower continental crust

Statement of significance

Magmatic sulfide deposits in exposed lower crustal rocks may be important future exploration targets. However, compared to well-understood upper crustal settings, little is known about the processes that produce sulfide deposits in the deep lithosphere. This study on the strongly metasomatized and mineralized Valmaggia pipe in the Ivrea-Verbano Zone (NW Italy) highlights the importance of mantle metasomatism in the formation of such deposits. We discuss where such metasomatic fluids originate, how they can reactivate/infiltrate pre-existing structures (pipes) that then allow for strongly focused mass transfer–and how this process can result in the formation of economically important magmatic sulfide mineralization.

Abstract

The lower crustal domain of the Ivrea-Verbano Zone (NW Italy) hosts five ~300-m-wide pipe-like ultramafic intrusions that are metasomatized and exhibit Ni-Cu-PGE sulfide mineralization. To better constrain the role of metasomatism in the ore genesis, we studied the best-preserved pipe at Valmaggia which was emplaced 249 Myrs ago. Phlogopite $^{40}Ar/^{39}Ar$ analyses show that the pipe was infiltrated by metasomatic fluids derived from the subcontinental lithospheric mantle (SCLM) in two pulses at ~208 Ma and ~189 Ma which introduced sulfides into the pipe. Consequently, the pipe repeatedly acted as a preferred path for mass transfer from the SCLM into the lower crust over >60 Myrs (i.e., emplacement to second metasomatic pulse). Uplifted block margins, such as the Ivrea-Verbano Zone, are potentially important exploration targets for magmatic sulfides. We argue that exploration strategies should focus on structures such as pipes that can focus metasomatic agents during ascent through the lithosphere.

1. Introduction

Lower crustal rocks may host significant magmatic sulfide deposits, but the mechanisms controlling the genesis and emplacement of mineralization in the lower crust are still not fully understood. For example, while metasomatism of the subcontinental lithospheric mantle (SCLM) has been proposed as an important precursor for the formation of some magmatic sulfide systems in overlying upper crustal settings (Fiorentini et al., 2018; Holwell et al., 2019; Locmelis et al., 2016) the origin and nature of mantle-derived metalliferous fluids, and the timescale over which re-fertilization of the commonly depleted SCLM occurs, remain poorly constrained.

Direct study of lower crustal sulfide deposits is permitted in the Ivrea-Verbano Zone (IVZ) in northwest Italy (Fig. 1), where rocks of the lower continental crust were uplifted during the Alpine

Orogeny from ~100 Ma onwards (e.g., Mehnert, 1975; Schmid 1993). The IVZ hosts five strongly metasomatized Permo-Triassic ultramafic pipes that are up to 300 m in diameter and were emplaced under lower crustal conditions (Fiorentini et al. 2002; Garuti et al. 2001; Locmelis et al., 2016; Sessa et al. 2017). Locmelis et al. (2016) proposed that the pipes initially formed as olivine cumulates with minor clinopyroxene, and were infiltrated by a late-stage hydrous melt and/or fluid which produced a secondary hydrous silicate assemblage dominated by pargasitic amphibole and phlogopite. The pipes host nodular-to-matrix Ni-Cu-PGE sulfide mineralization mostly along their margins, dominated by pyrrhotite, pentlandite and chalcopyrite, with ore grades up to 11.9 wt.% Cu, 10.7 wt.% Ni, and 5 ppm PGE (Zaccarini et al., 2014). Although these deposits are relatively small and only have been mined periodically between 1865 and 1943 (Fiorentini et al. 2002), they allow for insight into the poorly constrained processes that facilitate sulfide ore genesis in the lower crust. Locmelis et al. (2016) showed that the parental magma cannot explain the high Cu and Ni contents of the sulfide ore and suggested that a late-stage metasomatic event introduced metals into the pipes. Whereas Blanks et al. (2020) suggest that the association of sulfides and carbonates in the pipes reflects emplacement of a late CO_2-H_2O mineralizing fluid, this study focusses on the associated hydrous phases to inform on the nature and timing of this metasomatic event(s). For this purpose, we integrate new petrographic observations with mineral chemical data for primary clinopyroxene and secondary amphibole and mica (including $^{40}Ar/^{39}Ar$ ages of phlogopite) from the best-preserved IVZ pipe at Valmaggia.

2. Ivrea-Verbano Zone

The IVZ is an exposed cross-section of the continental lithosphere that is subdivided into the Mafic Complex, the Kinzigites, and the Mantle Peridotites (Fig. 1). The Mafic Complex formed from mantle-derived mafic magmas that underplated the basement of the Southern Alps at ~288-286 Ma (Mehnert, 1975; Rivalenti et al., 1984; Pin and Sills, 1986; Sinigoi et al., 1994; Peressini et al. 2007; Fiorentini et al., 2018). The Kinzigites are amphibolite-to-granulite facies rocks that structurally overlie the Mafic Complex (Bea & Montero, 1999; Schnetger, 1994), whereas the Mantle Peridotites are obducted slices of SCLM that crop out along the Insubric Line (Shervais and Mukasa, 1991; Hartmann and Wedepohl, 1993; Zanetti et al. 1999; Grieco et al. 2001). A series of metasomatized ultramafic pipes containing Ni-Cu-PGE sulfide mineralization were emplaced between ca. 287-249 Ma into the Mafic Complex and the Kinzigites (Garuti et al., 2001; Locmelis et al., 2016; Fiorentini et al., 2018; Fig. 1). Sessa et al. (2017) showed that the Valmaggia pipe, and by inference the other IVZ pipes, were metasomatized at P-T conditions between 680-870^{o}C and 4-8 kbar consistent with a metasomatic reaction of a peridotitic protolith at lower crustal conditions in extensional settings. The IVZ also hosts the ≥400 m thick and ≥3 km long La Balma-Monte Capio intrusion (LBMC), which contains Ni-Cu-PGE sulfide mineralization (Ferrario el al., 1983). However recent dating (Denyszyn et al., 2018; 200.1+/-0.5 Ma) suggests that this intrusion did not form as part of the IVZ, but instead represents a distal portion of the Central Atlantic Magmatic Province (CAMP).

2.1 The Valmaggia pipe

The Valmaggia pipe was described in Garuti et al. (2001), Fiorentini et al. (2002), Locmelis et al. (2016) and Sessa et al. (2017). The ~300-m-wide pipe is the youngest among the IVZ pipes and intruded the Mafic Complex at ~249 Ma (Locmelis et al., 2016). Its mineralogy reflects a multistage paragenetic history dominated by mm-sized olivine, cm-sized poikilitic amphibole (pargasite), symplectic spinel, phlogopite and orthopyroxene, with minor clinopyroxene and accessory carbonate and apatite. The pipe also contains nodular-to-blebby Ni-Cu-PGE sulfide mineralization (Fig. 2a-f). The pipe is rarely in direct contact with the Mafic Complex, but instead enveloped by a meter-wide, mottled rock which consists of mm- to cm-sized ultramafic enclaves (similar to the pipe assemblage) embedded in a sodic (An_{60-80}) plagioclase-rich matrix with accessory fine-grained Mg-biotite, amphibole and apatite (Fig. 2g). The mottled rock had been informally termed 'plagioclasite' by Garuti et al. (2001) to distinguish it from the similar-looking wall rock gabbro of the Mafic Complex.

3. Methodology

Silicate trace element analysis was performed at Curtin University (Perth, Australia) using a Resonetics RESOlution M-50A-LR connected to an Agilent 7700s quadrupole ICP-MS. Phlogopite geochronological stepwise heating $^{40}Ar/^{39}Ar$ analysis was performed at the University of Vermont Noble Gas Geochronology Laboratory and at the Western Australian Argon Isotope Facility at Curtin University. A detailed description of the methodology is presented as Supporting Information S1. $^{40}Ar/^{39}Ar$ analytical data are presented in S2 and new mineral chemistry data are presented in S3.

4. Results

Petrographic features of the Valmaggia pipe detailing the metasomatic past of the pipe are shown in Figs. 3a-f and 4a-c. Brown-green amphibole (pargasite) is ubiquitous. Clinopyroxene commonly contains inclusions of subhedral olivine and shows replacement by pargasite in the presence of (mostly accessory) plagioclase, which is generally in disequilibrium. (Fig. 3d, 4b). Orthopyroxene occurs as coarse-grained relict grains and as reaction coronas around mm-sized olivine (Fig. 3a-b). Phlogopite forms mm-sized lamellae frequently intergrown with amphibole, carbonate and sulfides (Fig. 3a-e-f). The mottled plagioclasite developed reaction coronas along the pipe margin (Fig. 4a) and amphibole-phlogopite reaction coronas around the ultramafic enclaves which are occasionally sulfide-rich (Fig. 4b-d). The replacement textures observed within the pipe and its margins are compatible with a two-stage paragenetic scheme involving "primary" peridotite phases and "secondary" hydrous silicates.

Clinopyroxene exhibits flat chondrite-normalized REE patterns and enriched primitive mantle-normalized patterns with depletions in compatible metals (Fig. 5a-b); grain portions less affected by amphibole replacement are lower in REE and most trace elements. Amphibole from the inner portions of the pipe has flat-to-convex chondrite-normalized REE patterns with maxima at Nd-Sm (Fig. 6a). Amphibole from the pipe margin and the enclaves display similar patterns, but with pronounced HREE depletion and Eu enrichment. Some amphiboles show a gradual color change from reddish-brown adjacent to replaced pyroxene to pale green with increasing distance (Fig. 3c). Reddish amphibole cores and greenish rims have similar REE patterns, but concentrations decrease toward the edges (Fig. 6b). Mantle-normalized patterns are overall similar, although some amphiboles from the pipe's interior are depleted in incompatible elements (Fig. 6c). Phlogopite from the pipe and accessory biotite from the plagioclasite have similar mantle-normalized trace element patterns (Fig. 7), although phlogopite is relatively depleted in incompatible elements and more enriched in compatible metals. The $^{40}Ar/^{39}Ar$ analyses of three samples yielded plateau ages (with 2σ errors quoted) of 209.4±5.1 Ma (L3-13, inner portion), 207.8±2.0 Ma (L2-12, inner portion), and 188.9±1.3 (I-7, margin; Fig. 8).

5. Discussion

5.1 Origin and emplacement of the late-stage hydrous melt

The metasomatic event discussed here likely played an important role in the formation of the Ni-Cu-PGE sulfide mineralization because (i) the parental magma was not enriched in chalcophile metals (Locmelis et al., 2016) and (ii) there is an ubiquitous spatial association between volatile-rich phases and sulfide mineralization, most notably along the margins of the pipe (Sessa et al., 2017).

The mottled plagioclasite that envelops the pipe (Figs. 2d, 9a-b), and reaction corona micro-textures (Figs. 3, 4), allow to determine how the metasomatic agent was emplaced. The mottled texture is notably similar to disequilibrium textures observed in mantle rocks affected by melt-rock interaction (Fig. 9c). The textural disequilibrium between clinopyroxene and amphibole is consistent with interaction between a peridotitic protolith and a more silica-rich (e.g., hydrous basaltic-andesitic; Grant & Harlov, 2018) metasomatic agent which promoted the recrystallization of clinopyroxene into amphibole, likely at ≤900°C and 4-8 kbar (*cf.* Sessa et al., 2017). Petrographic evidence for this metasomatic reaction is recorded by the pargasite color change from red (near clinopyroxene) to green (farther away) which also corresponds to a depletion in REE (Fig. 6b). Clinopyroxene records similar evidence for a metasomatic front as its REE contents increase with advanced degrees of replacement (Fig. 5a). Furthermore, REE partitioning coefficients between amphibole and clinopyroxene of ~2.9 (*cf.* S3) reflect chemical disequilibrium between primary and secondary phases, analogous to observations made for other ultramafic amphibole-rich rocks such as the Adamello batholith (Tiepolo et al. 2011). Based on these observations, we argue that the metasomatic fluid infiltrated the pipe along its margin, produced the mottled texture and triggered pervasive metasomatism that resulted in the widespread formation of the secondary hydrous assemblage. Because secondary amphibole and phlogopite display suprachondritic rather than intraplate Nb-Ti-Zr signatures (Fig. 10), it is inferred that the metasomatic fluid was likely derived from the SCLM. A lithospheric mantle source is also supported by S-isotopic studies of sulfides from the Valmaggia pipe (Garuti et al. 1986; Fiorentini et al., 2018). A mantle source is further in agreement with a recent model by Blanks et al. (2020) who investigated the carbon and oxygen isotopic signatures of carbonates associated with phlogopite and sulfides in the Valmaggia pipe. These authors suggested that the metasomatising agent involved a deuteric (i.e., late magmatic) CO_2-H_2O fluid with mantle-derived carbon which might have physically transported metal-rich sulfides through the lithosphere. In this scenario, the metal enrichment in the pipe's margin likely reflects (i) a metal-rich source region, and (ii) the highly reactive nature of the agent and assimilation of metals from wall-rock during ascent and upon emplacement.

5.2 The timing of metasomatism

$^{40}Ar/^{39}Ar$ analysis of pipe-hosted phlogopite, formed in response to the late-stage metasomatism, yielded ages of 188.9±1.3 Ma in the pipe's margin and 209.4±5.1 Ma and 207.8±2.0 Ma toward the central portion. The ages suggest that metasomatism occurred in (at least) two distinct pulses. In the IVZ, these ages are significantly younger than the inferred emplacement age of the Valmaggia pipe (249.1±0.2 Ma; Locmelis et al. 2016) and bracket the age of the emplacement of the CAMP-associated La Balma-Monte Capio Complex at 200.1±0.5 Ma (Denyszyn et al., 2018; Fig. 1). The phlogopite ages are also consistent with those of a suite of recently discovered carbonatite pipes emplaced in the IVZ (187±2.4 to 192±2.5 Ma; Galli et al., 2019; Fig. 1), zircon from chromitite layers in the metasomatized Finero mantle peridotite (~187 Ma; Zanetti et al., 2016), and zircon from the phlogopite peridotite unit of the Finero Complex that record a metasomatic event at 207.9 Ma (Grieco et al., 2001). A minor age peak at ~208 Ma was also observed by Malitch et al. (2017) in zircon from Finero chromitites at Rio Creves. It is noted that the phlogopite ages may not represent magmatic crystallization ages, but thermal resetting of earlier-crystallized phlogopite during later regional high-temperature events. For this interpretation to be valid, either discrete resetting events must have occurred in the IVZ to generate the different phlogopite ages, or the studied samples were variably/partially reset. However, considering that the Valmaggia pipe is only <300 m in diameter, thermal events that separately reset phlogopite in only small portions of the pipe are implausible. The coherence of the older ages from phlogopite from the interior of the pipe also argues against variable partial resetting. Therefore, the likeliest interpretation is that the $^{40}Ar/^{39}Ar$ ages reported here represent primary crystallization ages and thus record the migration of fluids from the SCLM into the overlying crust in two distinct pulses. This hypothesis is further supported by the U-Pb zircon ages reported by Grieco et al. (2001), Zanetti et al. (2016) and Galli et al. (2019) that highlight widespread metasomatic events in the IVZ during that period. In this framework, the Valmaggia pipe represents a structural pathway that repeatedly allowed for strongly focused mass transfer from the upper mantle into the lower crust during several regional magmatic/metasomatic events over a ~60 Myr interval, i.e., from the ~249 Ma ultramafic magmatism to the latest metasomatic pulse at ~189 Ma.

5.3 Implications for the formation of lower crustal magmatic sulfide systems

Although discoveries of magmatic sulfide deposits in exposed lower crustal rocks remain rare, it can be argued that such settings represent important future exploration targets owing to the decline of discoveries in upper crustal rocks (Schodde, 2017). While the IVZ does not contain giant Ni-Cu-PGE sulfide deposits, the mineralized pipes and La Balma - Monte Capio complex allow to better understand the processes that control ore genesis in the lower continental crust, which is an important step toward including such lower crustal rocks into exploration models. Moreover, such lower crustal deposits, if reworked and/or remolten, might be considered as potential lower crustal proto-ores and/or precursor ores to bigger ore deposits located in upper crustal settings (Holwell et al. 2019).

The new $^{40}Ar/^{39}Ar$ ages for the metasomatic event in the Valmaggia pipe bracket the 200 Ma age of the LMBC. This temporal link supports the model of Fiorentini et al. (2019), who put forward the hypothesis that the composition and metal endowment of the LBMC reflect mixing between a deeply sourced juvenile and relatively dry primitive CAMP magma with localized SCLM pods enriched in volatiles, metals, and sulfur (consistent with the composition of the IVZ pipes). In this model, the mineralized IVZ pipes and the LBMC intrusion represent different magmatic and/or metasomatic pulses that utilized the boundary between continental blocks as a preferred path for upward mass and heat transfer for at least 60 Myrs. The inferred genetic link between the mineralized pipes and LBMC is consistent with the recent model by Holwell et al. (2019) which showed that sulfide mineralization at different lithospheric depths represents local stalling points of the same translithospheric metallogenic continuum. The observation that the IVZ pipes exhibit the highest ore grades among all IVZ deposits (Zaccarini et al., 2014) likely reflects that the narrow pipe structure allowed for particularly focused mass transfer and thus efficient concentration of metals.

The scenario depicted here helps explain why ore deposits are not evenly distributed along lithospheric block margins, but instead form clusters along discrete segments (Begg et al., 2010; Fiorentini et al., 2018). Furthermore, our observations suggest that (1) uplifted continental block margins should be systematically included in future exploration models, and (2) exploration strategies should particularly focus on physical structures, such as pipes, that have the potential to concentrate metasomatic agents during their ascent from the SCLM.

Acknowledgements

M. L. acknowledges funding through the NSF CAREER award 1944552 “Investigating the source, transport and deposition of economically important metals in the lower continental crust”. M. M., M. F., S. C. and G. S. acknowledge support for LA-ICP-MS analyses from the Australian Research Council through Linkage Project LP120100668. Fred Jourdan is thanked for help with the phlogopite Ar/Ar analysis at Curtin University. This manuscript has greatly benefited from critical reviews by José María González-Jiménez, Benoit Saumur and one anonymous reviewer. We thank Klaus Mezger for the editorial handling. This is contribution #3 of the Missouri S&T MCTF research group and a publication of the O’Keefe Institute for Sustainable Supply of Strategic Minerals at Missouri University of Science and Technology.

Conflict of Interest

The authors declare no conflict of interest.

Data Availability Statement

The data that support the findings of this study are provided in the supplementary material

References

Bea, F., & Montero, P., 1999. Behavior of accessory phases and redistribution of Zr, REE, Y, Th, and U during metamorphism and partial melting of metapelites in the lower crust: an example from the Kinzigite Formation of Ivrea-Verbano, NW Italy. *Geochimica et Cosmochimica Acta,* **63(7–8)**, 1133-1153.

Begg, G. C., Hronsky, J. A. M., Arndt, N. T., Griffin, W. L., O'Reilly, S. Y., & Hayward, N., 2010. Lithospheric, Cratonic, and Geodynamic Setting of Ni-Cu-PGE Sulfide Deposits. *Economic Geology,* **105(6)**, 1057-1070.

Blanks, D. E., Holwell, D. A., Fiorentini, M. L., Moroni, M., Giuliani, A., Tassara, S., González-Jiménez, J. M., Boyce, A. J., Ferrari, E. (2020). Fluxing of mantle carbon as a physical agent for metallogenic fertilisation of the crust. Nature Communications. In press.

Denyszyn, S. W., Fiorentini, M. L., Maas, R., & Dering, G., 2018. A bigger tent for CAMP. *Geology,* ***46*(9)**, 823-826.

Ferrario, A., Garuti, G., Rossi, A., & Sighinolfi, G. P., 1983. Petrographic and metallogenic outlines of the "La Balma-M. Capio" ultramafic-mafic body (Ivrea-Verbano basic complex, NW Italian Alps). *In: Mineral Deposits of the Alps and of the Alpine Epoch in Europe. Springer, Berlin, Heidelberg,* pp. 28-40.

Fiorentini, M. L., & Beresford, S. W., 2008. Role of volatiles and metasomatized subcontinental lithospheric mantle in the genesis of magmatic Ni–Cu–PGE mineralization: insights from in situ H, Li, B analyses of hydromagmatic phases from the Valmaggia ultramafic pipe, Ivrea-Verbano Zone (NW Italy). *Terra Nova,* **20(5)**, 333-340.

Fiorentini, M. L., Denyszyn, S., Dering, G., Holwell, D., Blanks, D., Maas, R., Locmelis, M., LaFlamme, C., 2019. Reactivation and enrichment of a Gondwana margin Ni-Cu-PGE-Au-Te mineral system during the breakup of Pangea. *In: 15th Biennial Meeting of the Society for Geology applied to Mineral Deposit, Society for Geology Applied to Mineral Deposits: Glasgow, UK,* **2**, 524-527.

Fiorentini, M. L., Grieco, G., Ferrario, A., & Tunesi, A., 2002. Petrological and metallogenic outlines of the Valmaggia ultramafic pipe (Ivrea zone), NW Alps, Italy. *Periodico di Mineralogia,* **71(3)**, 219-239.

Fiorentini, M. L., LaFlamme, C., Denyszyn, S., Mole, D., Maas, R., Locmelis, M., Caruso, S., Bui, T.-H., 2018. Post-collisional alkaline magmatism as gateway for metal and sulfur enrichment of the continental lower crust. *Geochimica et Cosmochimica Acta,* **223**, 175-197.

Garuti, G., Bea, F., Zaccarini, F., & Montero, P., 2001. Age, Geochemistry and Petrogenesis of the Ultramafic Pipes in the Ivrea Zone, NW Italy. *Journal of Petrology,* **42(2)**, 433-457.

Garuti, G., Fiandri, P., & Rossi, A., 1986. Sulfide composition and phase relations in the Fe-Ni-Cu ore deposits of the Ivrea-Verbano basic complex (western Alps, Italy). *Mineralium Deposita,* **22**, 22-34.

Grant, T. B. & Harlov, D.E., 2018. The influence of NaCl-H2O fluids on reactions between olivine and plagioclase: An experimental study at 0.8 GPa and 800–900° C. *Lithos*, **323**, 78-90.

Grieco, G., Ferrario, A., von Quadt, A., Koeppel, V., & Mathez, E. A., 2001. The Zircon-Bearing Chromitites of the Phlogopite Peridotite of Finero (Ivrea Zone, Southern Alps): Evidence and Geochronology of a Metasomatized Mantle Slab. *Journal of Petrology,* **42(1)**, 89-101.

Hartmann, G., & Wedepohl, H. K., 1993. The composition of peridotite tectonites from the Ivrea Complex, northern Italy: Residues from melt extraction. *Geochimica et Cosmochimica Acta,* **57(8)**, 1761-1782.

Holwell, D. A., Fiorentini, M., McDonald, I., Lu, Y., Giuliani, A., Smith, D., Keith, M., Locmelis, M., 2019. A metasomatized lithospheric mantle control on the metallogenic signature of post-subduction magmatism. *Nature Communications,* **10(1)**, 3511.

Locmelis, M., Fiorentini, M. L., Rushmer, T., Arevalo Jr., R., Adam, J., & Denyszyn, S. W., 2016. Sulfur and metal fertilization of the lower continental crust. *Lithos,* **244**, 74-93.

Malitch, K. N., Belousova, E. A., Griffin, W.L., Badanina, I.Y., Knauf, V.V., O'Reilly, S.Y. & Pearson, N.J., 2017. Laurite and zircon from the Finero chromitites (Italy): New insights into evolution of the subcontinental mantle. *Ore Geology Reviews,* **90***,* pp.210-225.

Mehnert, K. R., 1975. The Ivrea Zone, a model of the deep crust. *Neues Jahrbuch fuer Mineralogie: Abhandlungen,* **125(2)**, 156-199.

Naldrett, A. J., 2004. Magmatic sulfide deposits: Geology, Geochemistry and Exploration. *Heidelberg, Springer, 728 p.*

Pec, M., Holtzman, B. K., Zimmerman, M. E., & Kohlstedt, D. L., 2017. Reaction Infiltration Instabilities in Mantle Rocks: an Experimental Investigation. *Journal of Petrology,* **58(5)**, 979-1003.

Peressini, G., Quick, J. E., Sinigoi, S., Hofmann, A. W., & Fanning, M., 2007. Duration of a large mafic intrusion and heat transfer in the lower crust: a SHRIMP U-Pb zircon study in the Ivrea-Verbano zone (Western Alps, Italy). *Journal of Petrology,* **48(6)**, 1185-1218.

Pin, C., & Sills, J. D., 1986. Petrogenesis of layered gabbros and ultramafic rocks from Val Sesia, the Ivrea Zone, NW Italy: trace element and isotope geochemistry. *Geological Society, London, Special Publications,* **24(1)**, 231-249.

Rivalenti, G., Rossi, A., Siena, F., & Sinigoi, S., 1984. The layered series of the Ivrea-Verbano igneous complex, Western Alps, Italy. *Tschermaks Mineralogische und Petrographische Mitteilungen,* **33**, 77-99

Schodde, R., 2017. Recent Trends and Outlook for Global Exploration. *In:* Prospectors & Developers Association of Canada (PDAC) Convention, Conference Proceedings, Toronto, Canada

Schnetger, B., 1994. Partial melting during the evolution of the amphibolite- to granulite-facies gneisses of the Ivrea Zone, northern Italy. *Chemical Geology,* **113(1–2)**, 71-101.

Sessa, G., Moroni, M., Tumiati, S., Caruso, S., & Fiorentini, M. L., 2017. Ni-Fe-Cu-PGE ore deposition driven by metasomatic fluids and melt-rock reactions in the deep crust: The ultramafic pipe of Valmaggia, Ivrea-Verbano, Italy. *Ore Geology Reviews,* **90**, 485-509.

Shervais, J. W., & Mukasa, S. B., 1991. The Balmuccia orogenic lherzolite massif, Italy. *Journal of Petrology,* **2***, 155-174*.

Sinigoi, S., Quick, J. E., Clemens-Knott, D., Mayer, A., Demarchi, G., Mazzucchelli, M., Negrini, L., Rivalenti, G., 1994. Chemical evolution of a large mafic intrusion in the lower crust, Ivren-Verbano Zone, northern Italy. *Journal of Geophysical Research,* **99**, 21575-21590.

Tiepolo, M., Tribuzio, R., & Langone, A., 2011. High-Mg Andesite Petrogenesis by Amphibole Crystallization and Ultramafic Crust Assimilation: Evidence from Adamello Hornblendites (Central Alps, Italy). *Journal of Petrology,* **52**, 1011-1045.

Zaccarini, F., Garuti, G., Fiorentini, M. L., Locmelis, M., Kollegger, P., & Thalhammer, O. A. R., 2014. Mineralogical hosts of platinum group elements (PGE) and rhenium in the magmatic Ni-Fe-Cu sulfide deposits of the Ivrea Verbano Zone (Italy): An electron microprobe study. *Neues Jahrbuch für Mineralogie - Abhandlungen: Journal of Mineralogy and Geochemistry,* **191(2**), 169-187.

Zanetti, A., Mazzucchelli, M., Rivalenti, G., & Vannucci, R., 1999. The Finero phlogopite-peridotite massif: an example of subduction-related metasomatism. *Contributions to Mineralogy and Petrology,* **134**, 107-122.

Zanetti, A., Giovanardi, T., Langone, A., Tiepolo, M., Wu, F.-Y., Dallai, L., & Mazzucchelli, M., 2016. Origin and age of zircon-bearing chromitite layers from the Finero phlogopite peridotite (Ivrea–Verbano Zone, Western Alps) and geodynamic consequences. *Lithos,* **262**, 58-74.

List of figure captions

FIGURE 1 Simplified geological map of the Ivrea–Verbano Zone showing the location of the known ultramafic pipes, the La Balma – Monte Capio Intrusion, Mantle Peridotites, and carbonatite pipes near the study area (inset B). Modified from Fiorentini and Beresford (2008) and Locmelis et al. (2016).

FIGURE 2 Textural features observed in hand samples from the Valmaggia ultramafic pipe including its sulfide mineralization. a, b) Coarse-grained nodular sulfide mineralization in the pipe's interior that is dominated by amphibole, olivine, pyroxenes, phlogopite and minor whitish plagioclase pockets. c) Nodular sulfide mineralization along the pipe's margin near the contact with the mottled plagioclasite. d) Sulfide aggregate including pyrrhotite and pentlandite, accessory chalcopyrite and magnetite, intergrown with carbonate (large aggregate in the oval zone) and silicates (reflected light micrograph). e) Pyrrhotite and pentlandite including a bleb of Pt-Pd-rich Ni-Bi telluride (reflected light micrograph). f) Pt-Pd-rich Ni-Bi telluride bleb in pyrrhotite near the margin of a coarse-grained sulfide nodule (backscattered scanning electron microscope image). g) Blebby to finely disseminated sulfides in the darkish pipe rock within the ultramafic enclaves within the adjacent plagioclasite. The inset is a transmitted light thin section image depicting sulfide blebs rimmed by amphibole. Labels: amph: amphibole, opx: orthopyroxene, spin: spinel, plag: plagioclase, carb: carbonate, sulf: sulfide aggregate, po: pyrrhotite, pn: pentlandite, cpy: chalcopyrite, mag: magnetite.

FIGURE 3 Representative transmitted light images of thin sections from the inner portion of the Valmaggia pipe. a) Coarse-grained orthopyroxene showing incipient replacement by amphibole and phlogopite (sample L3-7-5). b) Reaction corona of orthopyroxene around olivine within poikilitic amphibole (sample L3-13-1). c) Poikilitic amphibole showing gradual change from brown to pale-green due to progressive metasomatic replacement. Amphibole hosts and spinel symplectites (sample L3-13-2). d) Remnant of a coarse-grained clinopyroxene intergrown with subhedral olivine and partially replaced by amphibole; also shown are orthopyroxene coronas between olivine and amphibole (sample L2-16-1). e) Phlogopite lamellae intergrown with sulfide and olivine embedded in an amphibole oikocryst (sample L3-7-5). f) Phlogopite lath intergrown with carbonate, amphibole and orthopyroxene in a reaction corona around olivine (sample L3-7-5). All photos were taken at plane polarized light except b), c) and f). Abbreviations: amph: amphibole, oliv: olivine, cpx, clinopyroxene, opx: orthopyroxene, plag: plagioclase, phlog: phlogopite, sulf: sulfide, spin: spinel.

FIGURE 4 Representative transmitted light images of thin sections from the marginal portions of the Valmaggia pipe and the ultramafic enclaves in the plagioclasite. a) Pipe-plagioclasite contact zone displaying symplectite reaction coronas with greenish pargasite amphibole and spinel (sample L2-12). b) Coronitic texture of a clinopyroxene-rich ultramafic enclave: clinopyroxene grains include olivine and display incipient replacement by amphibole along both cleavage plans and rims in contact with plagioclase (sample L2-14-1). c) Deeply reacted sulfide-bearing enclave with olivine remnants overgrown by orthopyroxene coronas and embedded in amphibole rimmed by spinel symplectites (sample L2-15c). d) Deeply reacted enclave with mm-sized phlogopite intergrown with amphibole containing orthopyroxene and spinel symplectites (sample L3-7). All photos were taken at plane polarized light. Labels: amph: amphibole, oliv: olivine, cpx, clinopyroxene, opx: orthopyroxene, plag: plagioclase, phlog: phlogopite, sulf: sulfide, spin: spinel.

FIGURE 5 (a) Chondrite-normalized REE and (b) primitive mantle-normalized trace element patterns with clinopyroxene partly replaced by amphibole in the Valmaggia pipe. C1 chondrite and primitive mantle values are from Lyubetskaya and Korenaga (2007).

FIGURE 6 (a) Chondrite-normalized REE composition of amphibole. (b) Chondrite-normalized REE composition of a zoned amphibole from a red core to a greenish margin. (c) Primitive mantle-normalized minor and trace element composition of amphibole. Primitive mantle and C1-chodrite values are from Lyubetskaya and Korenaga (2007).

FIGURE 7 Primitive mantle-normalized minor and trace element composition of micas (phlogopite, biotite). Primitive mantle values are from Lyubetskaya and Korenaga (2007).

FIGURE 8 Cumulative ^{39}Ar step heating spectra for phlogopite from the Valmaggia pipe. All phlogopite ages were calculated using the decay constant of Renne et al. (2010) and the Fish Canyon sanidine standard (28.305 Ma ±0.13%); Plateau ages were calculated using the mean of all of the plateau steps and are presented at the 2-σ level.

FIGURE 9 a) Representative photographs of hand samples from the Valmaggia pipe with the contact between the darkish pipe rock and plagioclasite and b) the mottled plagioclasite texture, where disseminated to blebby sulfides often occur. c) Back scattered electron images of melt-rock reaction interface obtained during reaction infiltration experiments by Pec et al. (2017) involving peridotite and basaltic melt, for comparison with the mottled plagioclasite and the reaction corona textures of the ultramafic enclaves (see Fig. 2g and 4a-d). The experiments by Pec et al. (2017) simulated the effects of reaction infiltration instability (or reaction porous flow) caused by percolating melts during melt-rock reaction involving mantle rocks for anhydrous systems at 1200-1250°C. It is noted that the amphibole-dominated, hydrous reaction assemblage at Valmaggia developed at lower temperatures (below 900 °C at 4 to 8 kbar; Sessa et al., 2017).

FIGURE 10 (a) Nb vs. Ti, (b) Nb vs. Zr, (c) Ti/Nb vs. Zr/Nb, and (d) Ti/Zr vs. Zr/Nb in amphibole and phlogopite from the Valmaggia pipe. The data are compared to different compositions typical of amphibole and phlogopite from mantle wedges above subduction zones and intraplate settings after Coltorti et al. (2007) who demonstrated that suprasubduction amphibole is commonly depleted in Nb with suprachondritic Ti/Nb and Zr/Nb ratios, owing to the low solubility of Nb in hydrous fluids which results generation of Nb-depleted fluids above subduction zones. Conversely, intraplate amphibole is enriched in Nb, with subchondritic Ti/Nb and Zr/Nb ratios. Phlogopite shows similar characteristics, but less pronounced as it generally does not incorporate the large spectrum of trace elements observed in amphibole.

Supplementary files

S1 Methodology

S2 $^{40}Ar/^{39}Ar$ Data

S3 Mineral chemistry data

Figure 1

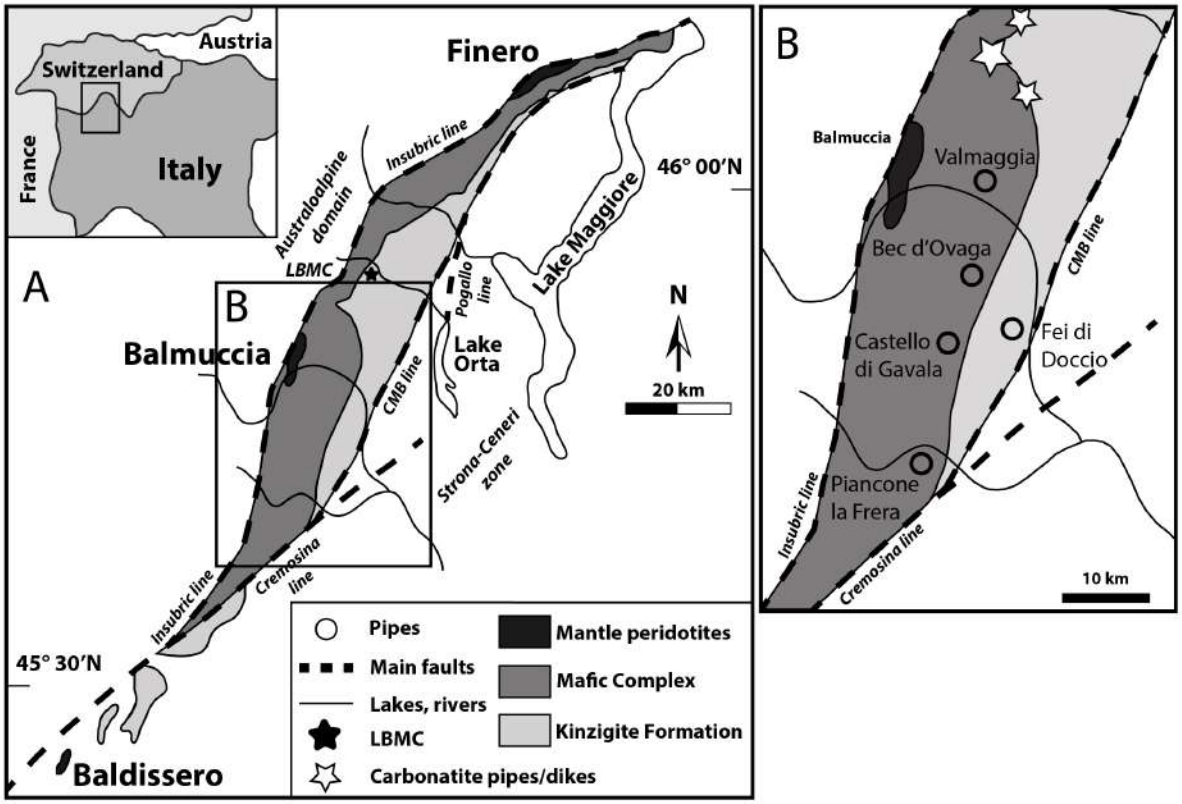

Austria
Switzerland
France
Italy
Finero
Insubric line
Australoalpine domain
46° 00'N
Lake Maggiore
LBMC
Pogallo line
A
B
Balmuccia
Lake Orta
CMB line
N
20 km
Strona-Ceneri zone
Cremosina line
Insubric line
45° 30'N
Baldissero
Pipes
Main faults
Lakes, rivers
LBMC
Carbonatite pipes/dikes
Mantle peridotites
Mafic Complex
Kinzigite Formation
B
Balmuccia
Valmaggia
Bec d'Ovaga
Castello di Gavala
Fei di Doccio
CMB line
Piancone la Frera
Insubric line
Cremosina line
10 km

Figure 2

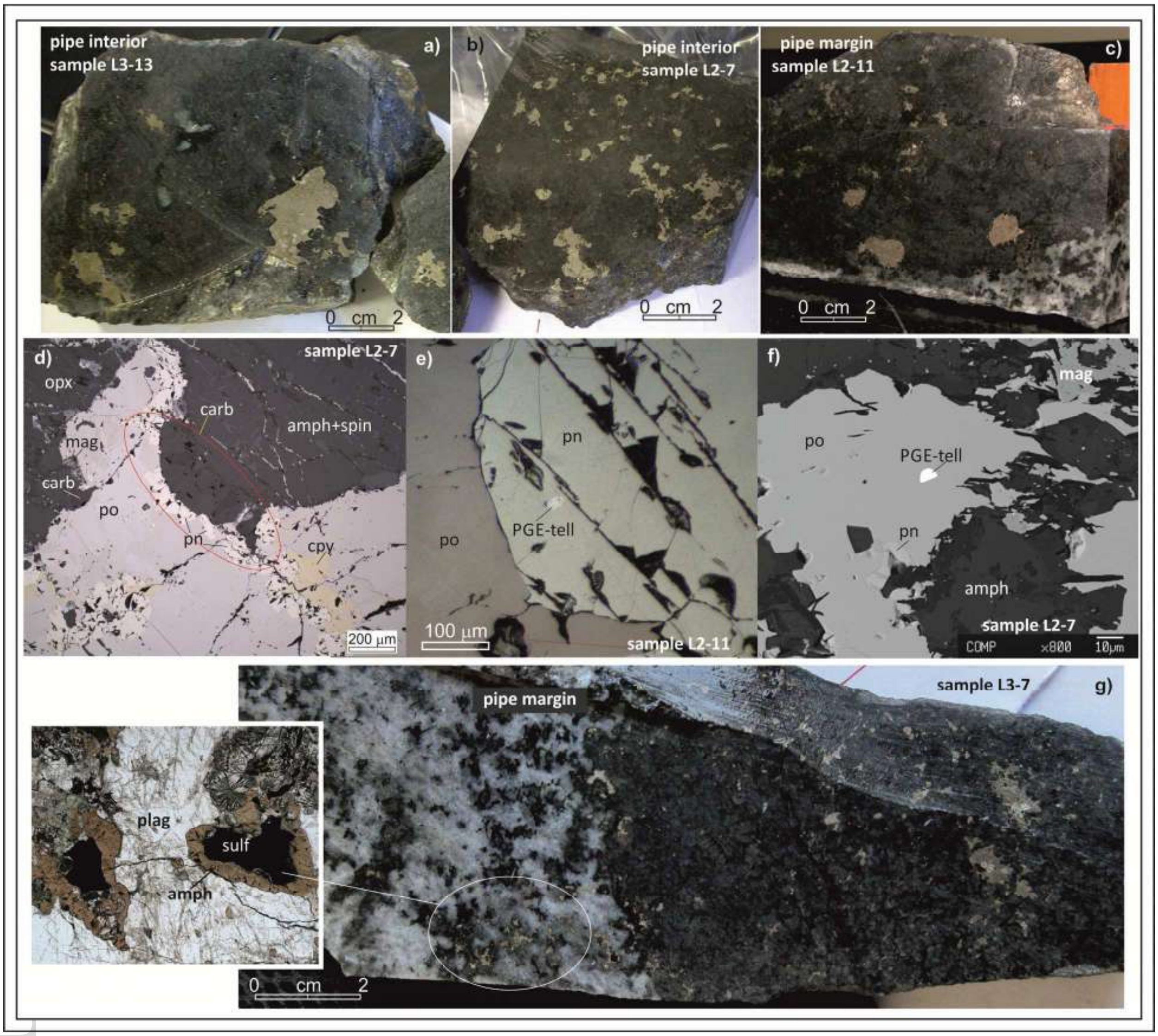
pipe interior
sample L3-13
a)
b)
pipe interior
sample L2-7
pipe margin
sample L2-11
c)
0 cm 2
0 cm 2
0 cm 2
d)
sample L2-7
opx
carb
amph+spin
mag
carb
po
pn
cpy
200 µm
e)
pn
po
PGE-tell
100 µm
sample L2-11
f)
mag
po
PGE-tell
pn
amph
sample L2-7
COMP ×800 10µm
pipe margin
sample L3-7
g)
plag
sulf
amph
0 cm 2

Figure 3

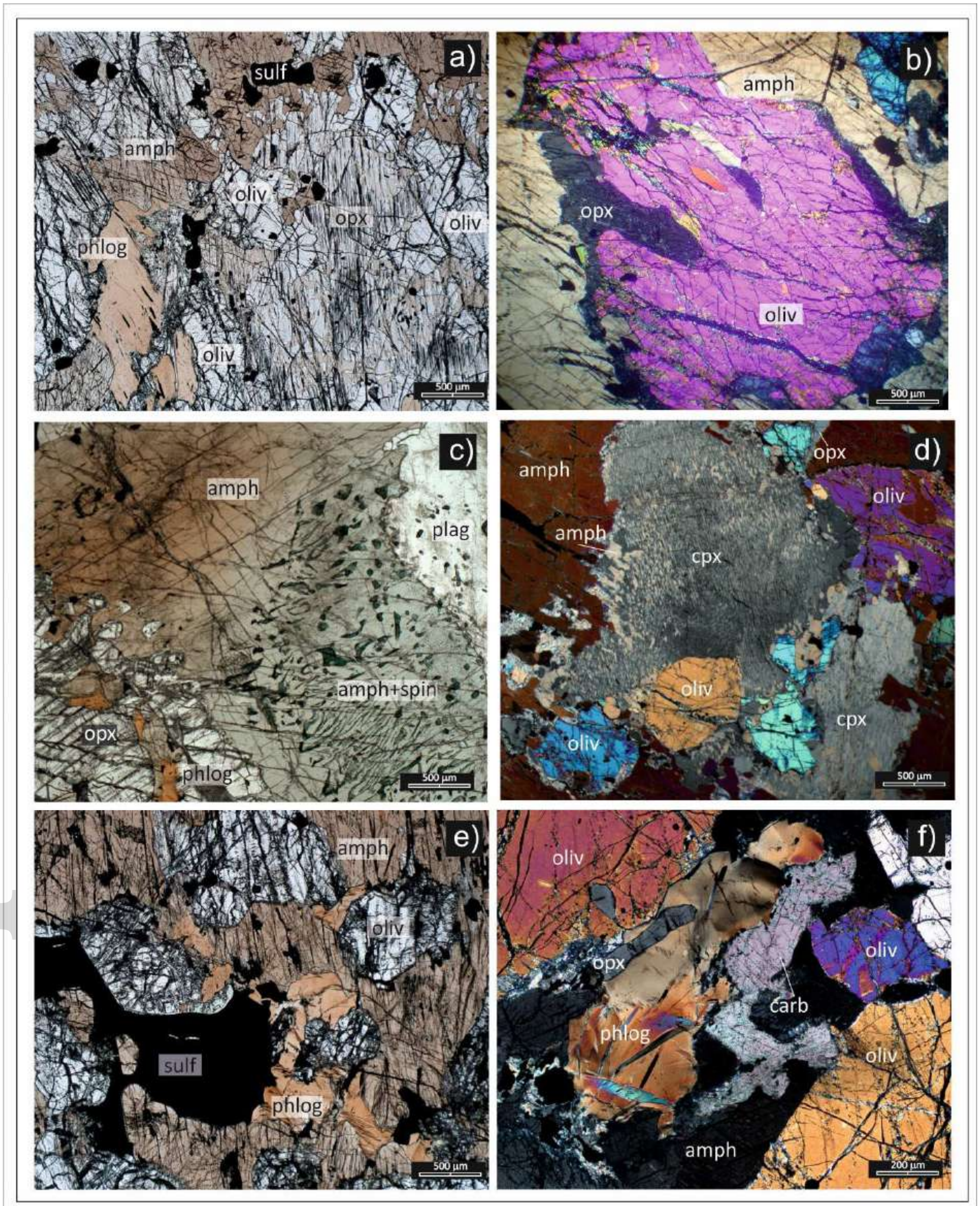
a)
sulf
amph
oliv
opx
oliv
phlog
oliv
500 µm
b)
amph
opx
oliv
500 µm
c)
amph
plag
amph+spin
opx
phlog
500 µm
d)
opx
amph
oliv
amph
cpx
oliv
cpx
oliv
500 µm
e)
amph
oliv
sulf
phlog
500 µm
f)
oliv
opx
oliv
carb
phlog
oliv
amph
200 µm

Figure 4

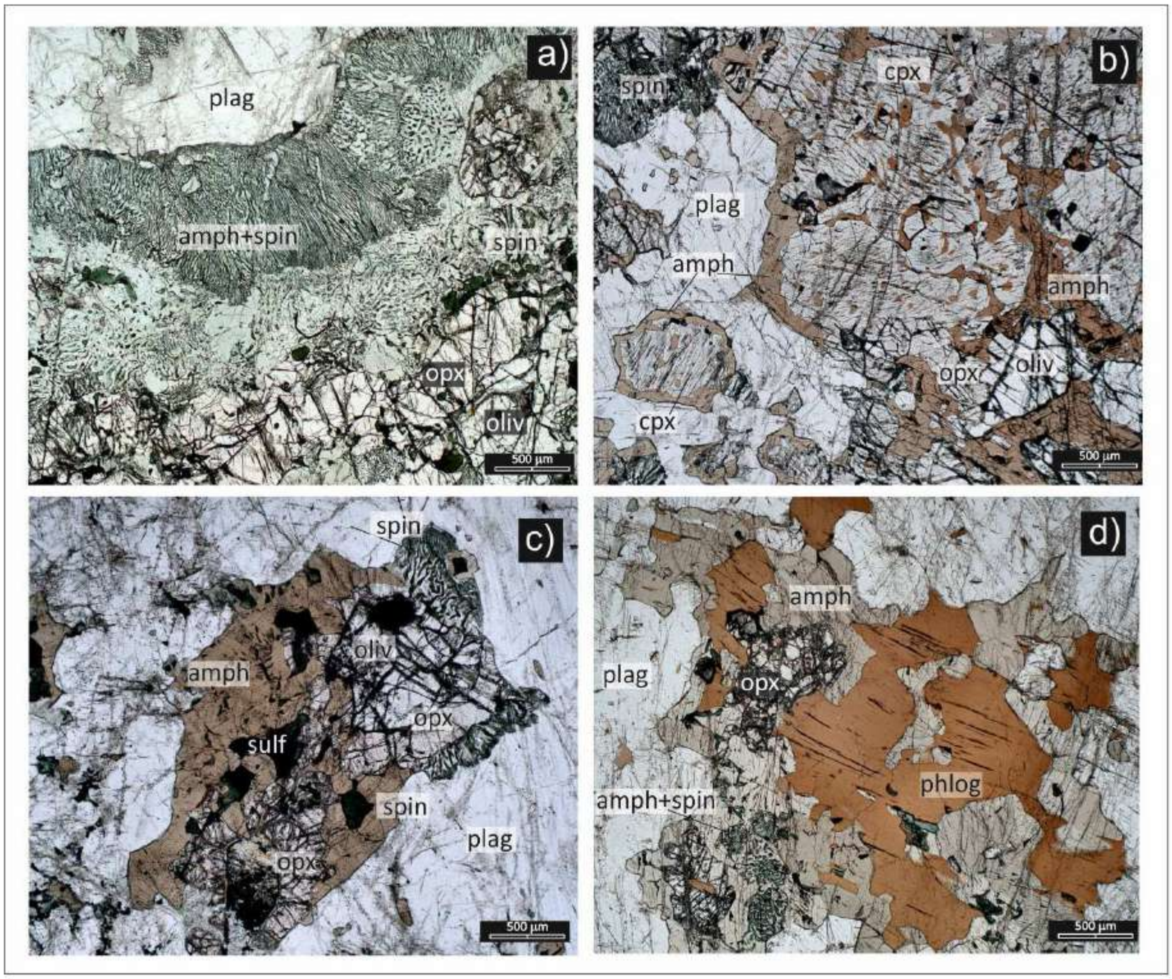
a)
plag
amph+spin
spin
opx
oliv
500 µm
b)
spin
cpx
plag
amph
amph
opx
oliv
cpx
500 µm
c)
spin
amph
oliv
opx
sulf
spin
plag
opx
500 µm
d)
amph
plag
opx
amph+spin
phlog
500 µm

Figure 5

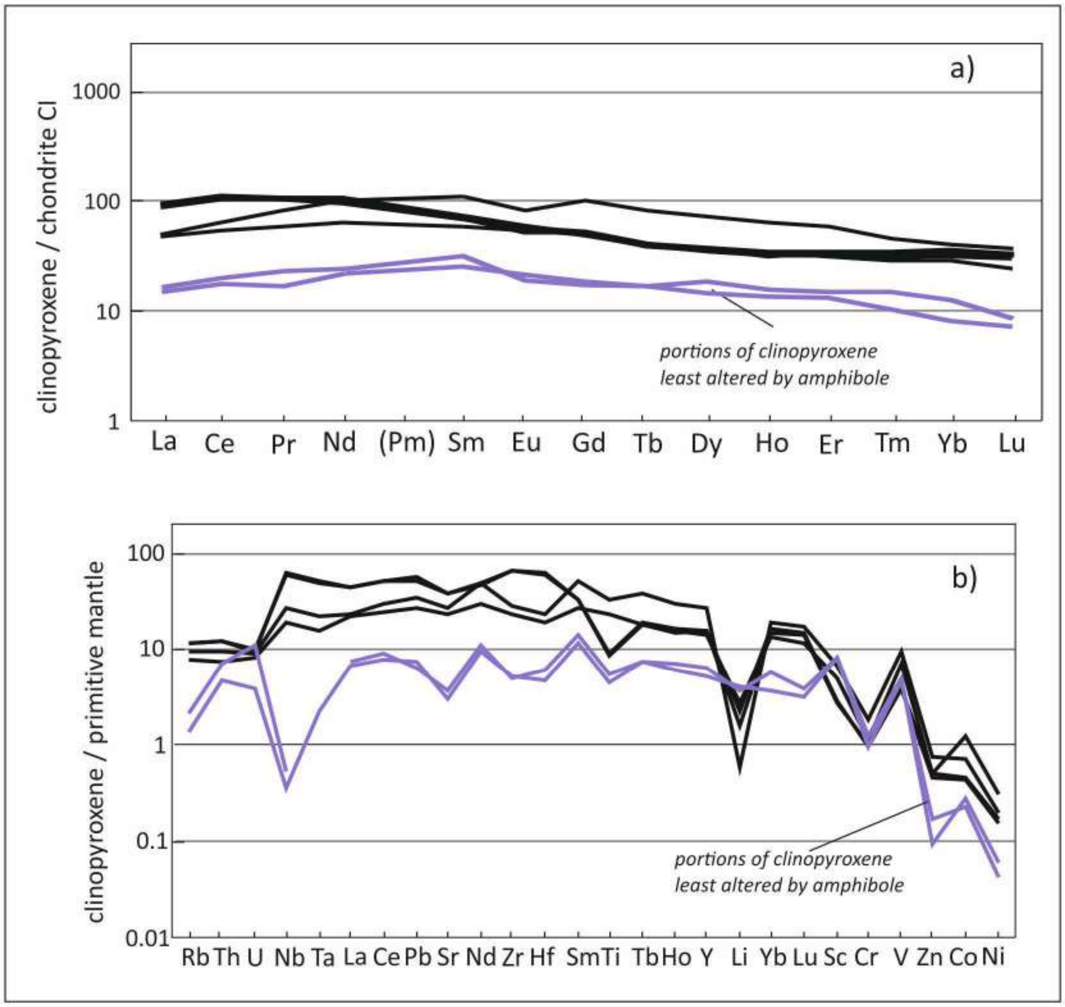
a)
clinopyroxene / chondrite CI
1000
100
10
1
La Ce Pr Nd (Pm) Sm Eu Gd Tb Dy Ho Er Tm Yb Lu
portions of clinopyroxene
least altered by amphibole
b)
clinopyroxene / primitive mantle
100
10
1
0.1
0.01
Rb Th U Nb Ta La Ce Pb Sr Nd Zr Hf Sm Ti Tb Ho Y Li Yb Lu Sc Cr V Zn Co Ni
portions of clinopyroxene
least altered by amphibole

Figure 6

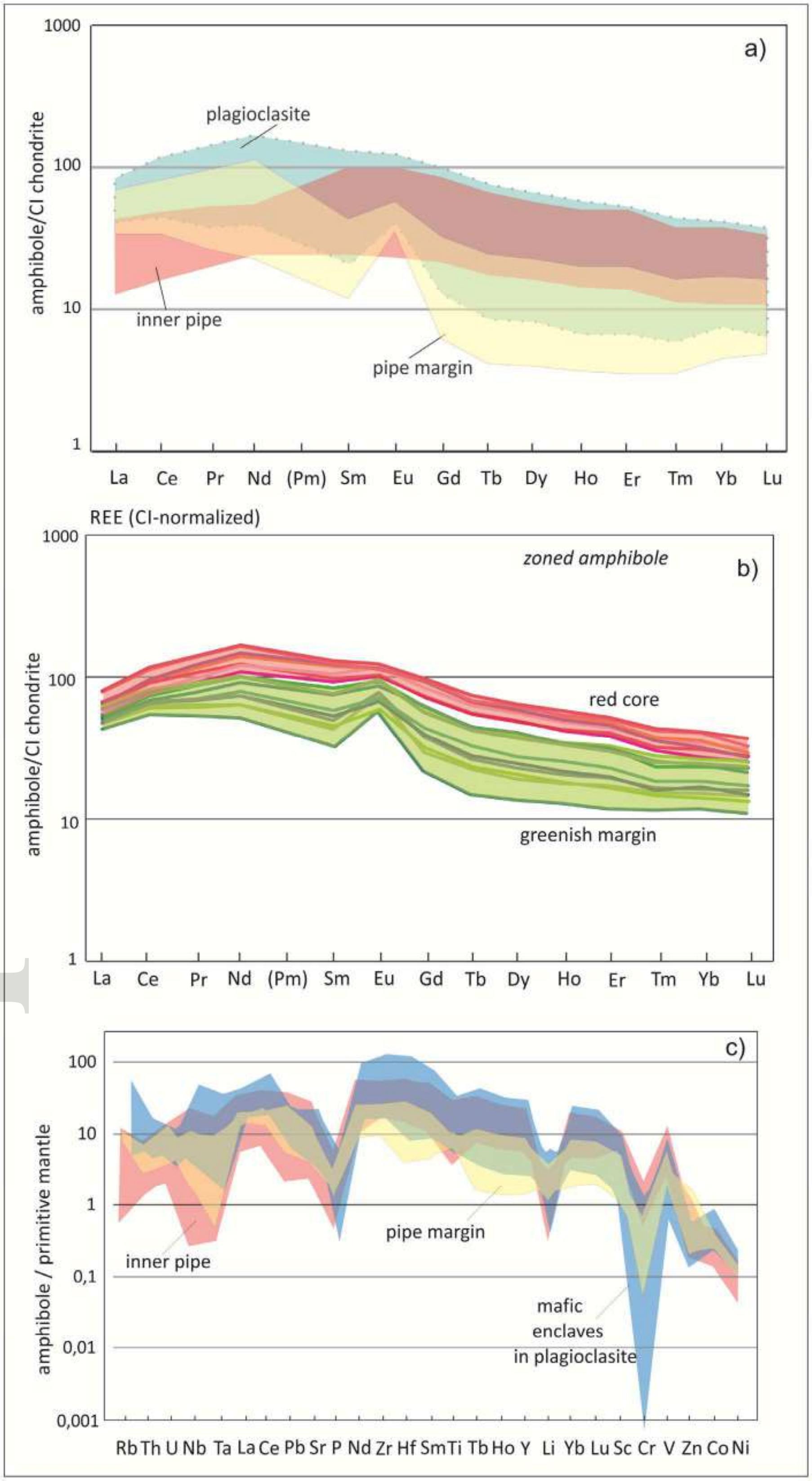
a)
1000
100
10
1
amphibole/CI chondrite
plagioclasite
inner pipe
pipe margin
La Ce Pr Nd (Pm) Sm Eu Gd Tb Dy Ho Er Tm Yb Lu
REE (CI-normalized)
b)
zoned amphibole
red core
greenish margin
La Ce Pr Nd (Pm) Sm Eu Gd Tb Dy Ho Er Tm Yb Lu
c)
100
10
1
0,1
0,01
0,001
amphibole / primitive mantle
inner pipe
pipe margin
mafic
enclaves
in plagioclasite
Rb Th U Nb Ta La Ce Pb Sr P Nd Zr Hf Sm Ti Tb Ho Y Li Yb Lu Sc Cr V Zn Co Ni

Figure 7

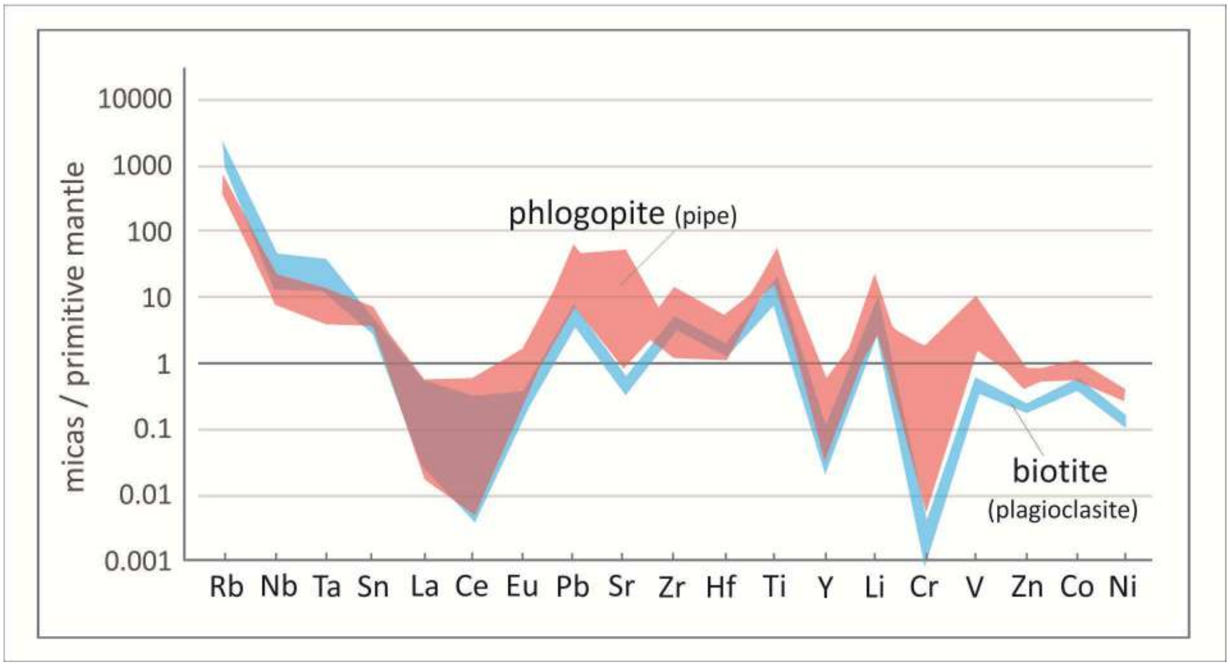
micas / primitive mantle
10000
1000
100
10
1
0.1
0.01
0.001
phlogopite (pipe)
biotite
(plagioclasite)
Rb Nb Ta Sn La Ce Eu Pb Sr Zr Hf Ti Y Li Cr V Zn Co Ni

Figure 9

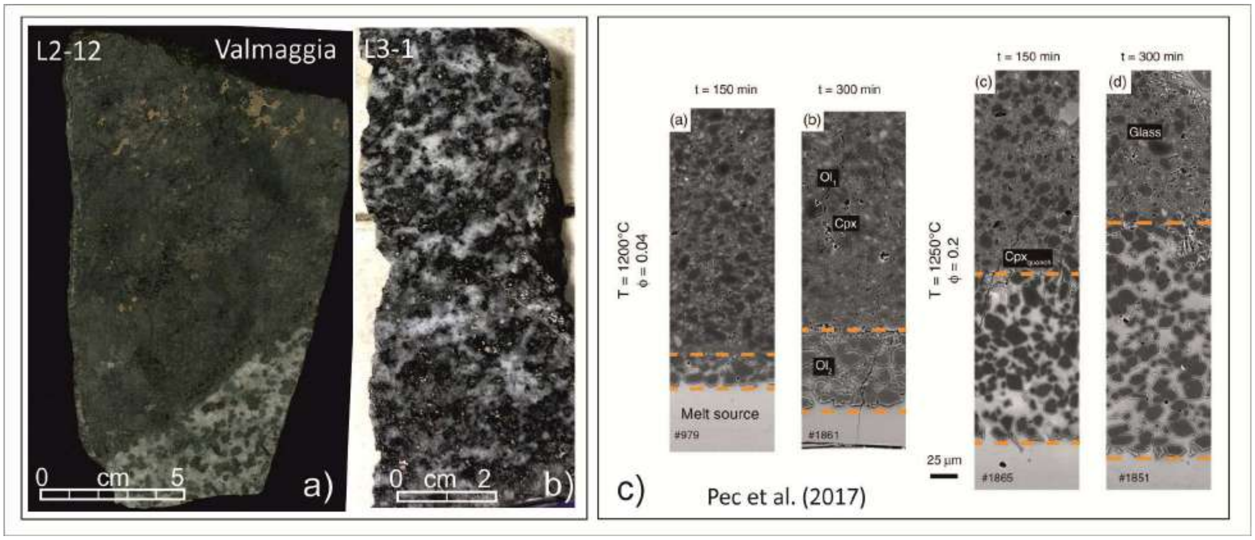
L2-12
Valmaggia
L3-1
0 cm 5
a)
0 cm 2
b)
c)
Pec et al. (2017)
t = 150 min
t = 300 min
(a)
(b)
(c)
(d)
T = 1200°C
ϕ = 0.04
T = 1250°C
ϕ = 0.2
Ol
Cpx
Glass
Melt source
#979
#1861
#1865
#1851
25 µm

Figure 10

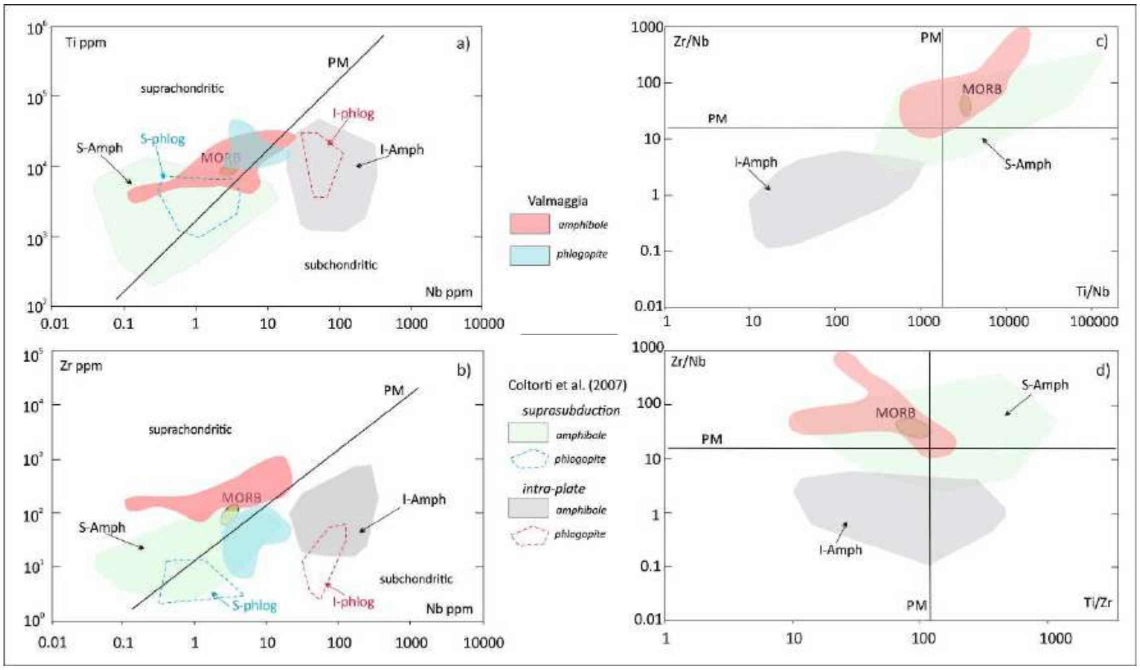
Ti ppm
a)
PM
suprachondritic
I-phlog
S-phlog
S-Amph
MORB
I-Amph
subchondritic
Nb ppm
Valmaggia
amphibole
phlogopite
Zr/Nb
PM
c)
MORB
PM
I-Amph
S-Amph
Ti/Nb
Zr ppm
b)
PM
suprachondritic
MORB
I-Amph
S-Amph
S-phlog
I-phlog
subchondritic
Nb ppm
Coltorti et al. (2007)
suprasubduction
amphibole
phlogopite
intra-plate
amphibole
phlogopite
Zr/Nb
d)
S-Amph
MORB
PM
I-Amph
PM
Ti/Zr